Electronic Supplementary Material (ESI) for Nanoscale.

Supplementary Information for

Manipulation of up-conversion emission in $NaYF_4$ core@shell nanoparticles doped by Er^{3+}, Tm^{3+}, or Yb^{3+} ions by excitation wavelength — three ions—plenty of possibilities

Tomasz Grzyb[1]*, Piotr Kamiński[1], Dominika Przybylska[1], Artur Tymiński[1], F. Sanz-Rodríguez[2], Patricia Haro Gonzalez[2]

[1]Department of Rare Earths, Faculty of Chemistry, Adam Mickiewicz University in Poznań, Uniwersytetu Poznańskiego 8, 61-614 Poznań, Poland

[2]Fluorescence Imaging Group, Departamento de Física de Materiales e Instituto Nicolás Cabrera, Facultad de Ciencias, Universidad Autónoma de Madrid, Campus de Cantoblanco, Madrid 28049, Spain

**E-mail: tgrzyb@amu.edu.pl*

1. Experimental

Synthesis of rare earth acetates

For the synthesis of 10 mmol of rare earth acetate, 5 mmol of rare earth oxide was dissolved in 40 ml of an aqueous solution of acetic acid (40% in demineralised water). The mixture was heated at 85°C for 16 h under a reflux condenser at atmospheric pressure. Then, the solution was cooled to room temperature under the flow of pure nitrogen and was filtered. Unreacted acid was evaporated using a rotary evaporator (Heidolph) at 50°C, with vacuum around 50 mbar, to near dryness (for around 1 h). Then, the obtained rare earth acetate was cleaned by dissolution in an aqueous acetic acid solution (80%). For every 1 mmol of rare earth oxide, 1.1–1.4 ml of acetic acid solution was used. (The exact amount of solution depended on the type of rare earth acetate, with the smallest volume applied to the dissolution of yttrium acetate and the biggest volume for the dissolution of thulium acetate.) Then, the solution was put into a three-neck flask and

connected to a reflux condenser. The solution was heated to 85°C under nitrogen atmosphere, and acetic acid (≥99%) was added to the solution by funnel during cooling. The volume of concentrated, dropped acetic acid was assumed to be the same as the heated aqueous rare earth acetic acid solution. Next, the solution was heated under nitrogen atmosphere at 120°C for 2 h. The final acetate was obtained after cooling the solution to room temperature under nitrogen atmosphere. This solution was evaporated using a rotary evaporator (Heidolph) at 50°C (around 25 mbar) until the acetate was dry (for around 4 h). The amount of physically adsorbed water was estimated using thermogravimetric analysis (TGA). The amount of adsorbed water in acetates were in the range 1-4 %, i.e. 3.79% in the case of erbium acetate, 3.06% in yttrium acetate, 1.72% in ytterbium acetate, 0.98% in thulium acetate.

2. Structure and morphology

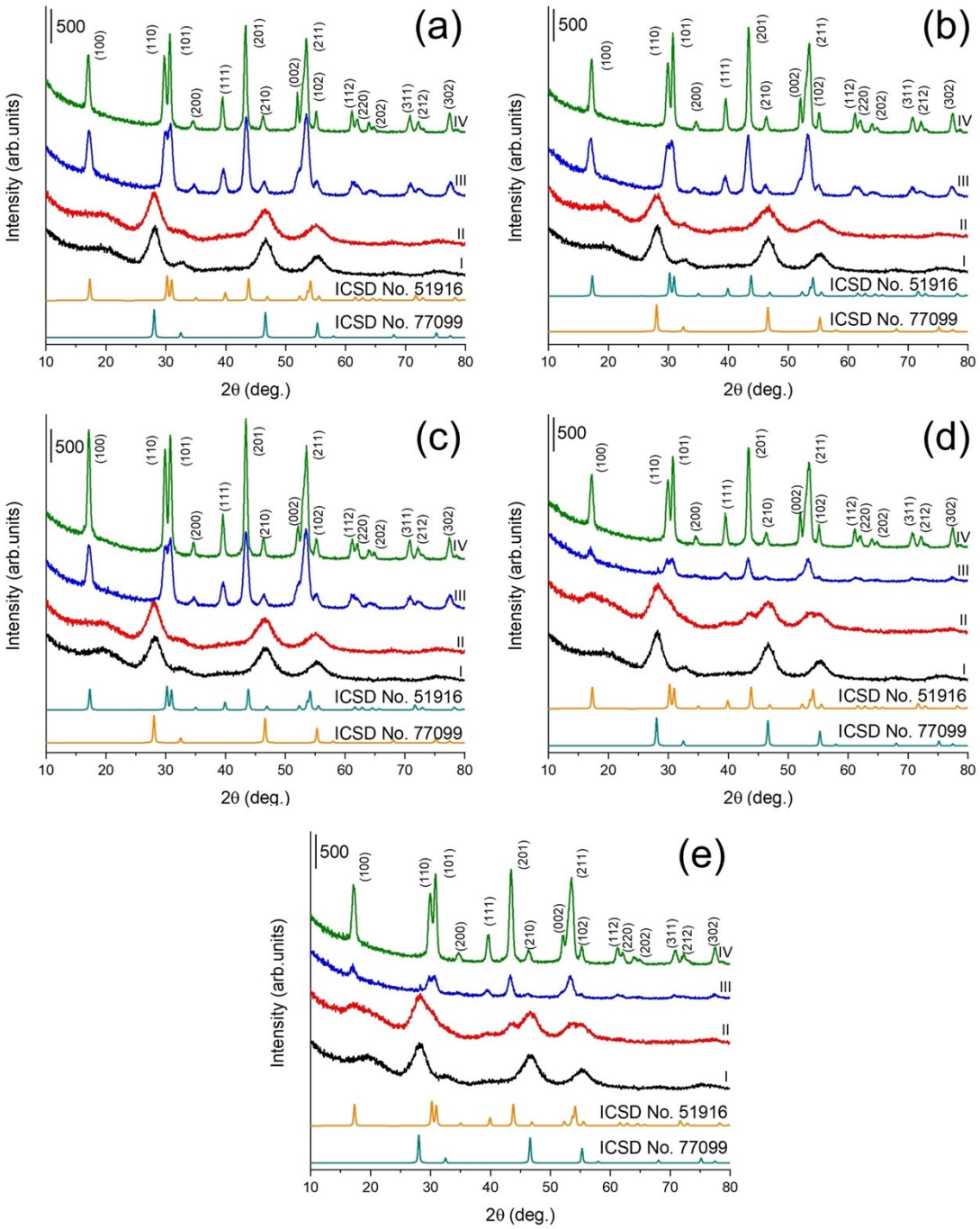

Fig. S1 X-ray diffraction (XRD) patterns of the synthesised fluorides: (a) $NaYF_4$:2%Tm^{3+}@$NaYF_4$, (b) $NaYF_4$:2%Tm^{3+},5%Er^{3+}@$NaYF_4$, (c) $NaYF_4$:2%Tm^{3+}@$NaYF_4$:5%Er^{3+}, (d) $NaYF_4$:18%Yb^{3+},2%Tm^{3+}@$NaYF_4$, and (e) $NaYF_4$:18%Yb^{3+},2%Tm^{3+}@$NaYF_4$:5%Er^{3+} and their forms, I: α-shell, II: α-core, III: β-core, and IV: β-core@β-shell.

XRD was applied to determine the average crystallite size, according to the Scherrer method.[1] Notably, the term “average crystallite size” is not synonymous with “average particle size” because XRD is sensitive to the crystallite size inside the particles. From the well-known Scherrer formula, the average crystallite size, *L*, is:

$$L = \frac{K\lambda}{\beta cos\theta} \qquad (1)$$

where λ is the X-ray wavelength in nanometres (nm); β is the peak width of the diffraction peak profile at half maximum height, resulting from small crystallite size, in radians; and K is a constant related to crystallite shape, normally taken as 0.9.

Table S1 The average size of crystallites with hexagonal structure, calculated using the Scherrer formula and determined from transmission electron mictroscopy TEM images and dynamic light scattering DLS measurements.

Sample	**Average size (nm)**		
	Scherrer	TEM	DLS
$NaYF_4$:2%Tm^{3+}	9.5 ± 0.6	10.0 ± 1.4	12.4 ± 3.0
$NaYF_4$:2%Tm^{3+}@$NaYF_4$	17.8 ± 2.0	18.4 ± 3.2	12.6 ± 2.7
$NaYF_4$:2%Tm^{3+}@$NaYF_4$:5%Er^{3+}	14.9 ± 1.1	12.2 ± 3.8	25.8 ± 5.3
$NaYF_4$:2%Tm^{3+},5%Er^{3+}	8.4 ± 1.1	5.4 ± 0.8	12.4 ± 3.0
$NaYF_4$:2%Tm^{3+},5%Er^{3+}@$NaYF_4$	15.8 ± 1.5	19.4 ± 2.9	11.6 ± 2.8
$NaYF_4$:18%Yb^{3+},2%Tm^{3+}	9.5 ± 1.4	7.1 ± 1.3	11.7 ± 2.8
$NaYF_4$:18%Yb^{3+},2%Tm^{3+}@$NaYF_4$	16.1 ± 1.8	14.4 ± 2.1	26.8 ± 5.7
$NaYF_4$:18%Yb^{3+},2%Tm^{3+}@$NaYF_4$:5%Er^{3+}	12.3 ± 0.9	15.9 ± 2.2	17.0 ± 3.8

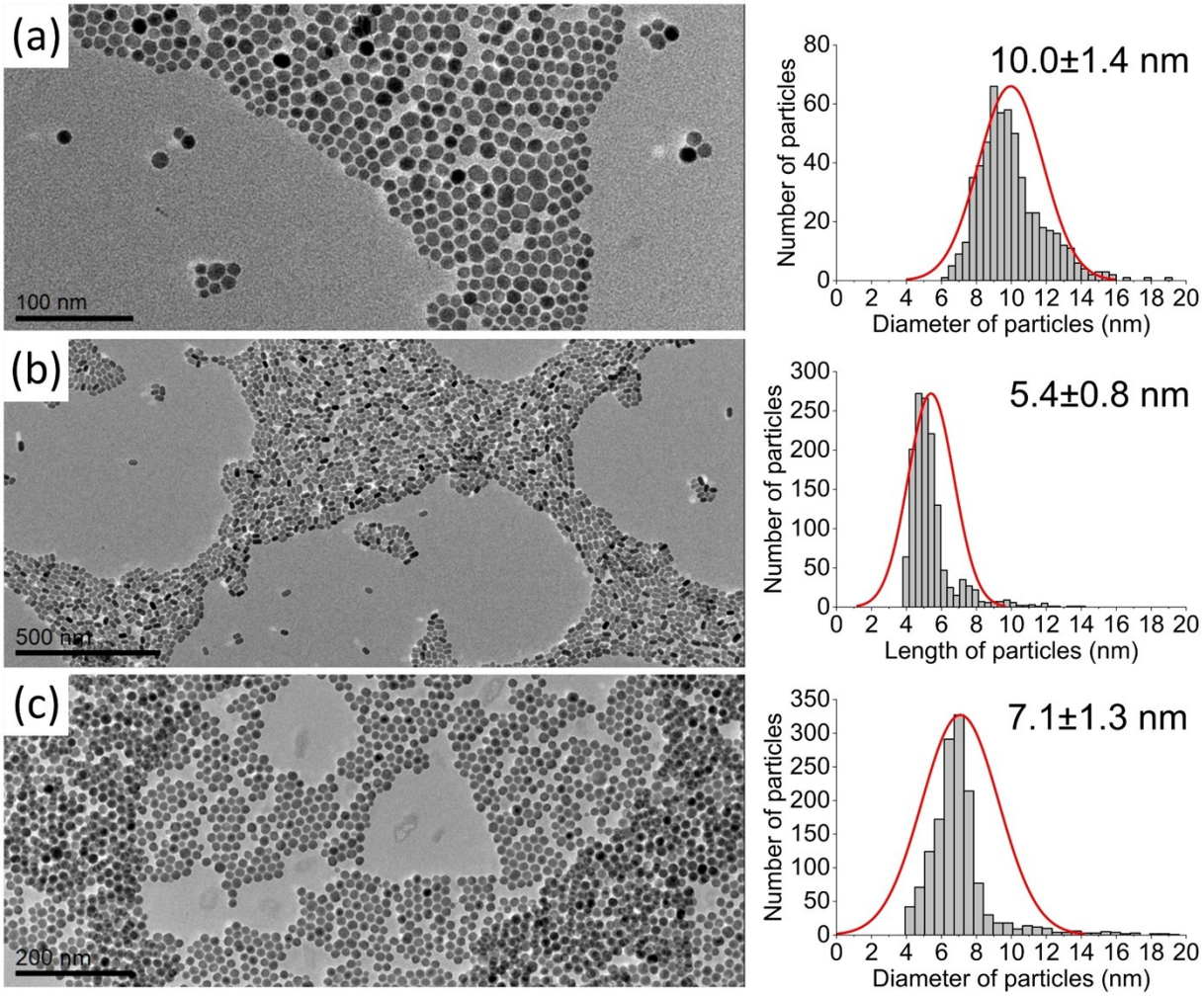

Fig. S2 TEM images (left) recorded for (a) β-$NaYF_4$:2%Tm^{3+}; (b) β-$NaYF_4$:2%Tm^{3+},5%Er^{3+}; and (c) β-$NaYF_4$:18%Yb^{3+},2%Tm^{3+} and calculated on their basis NPs sizes' distributions.

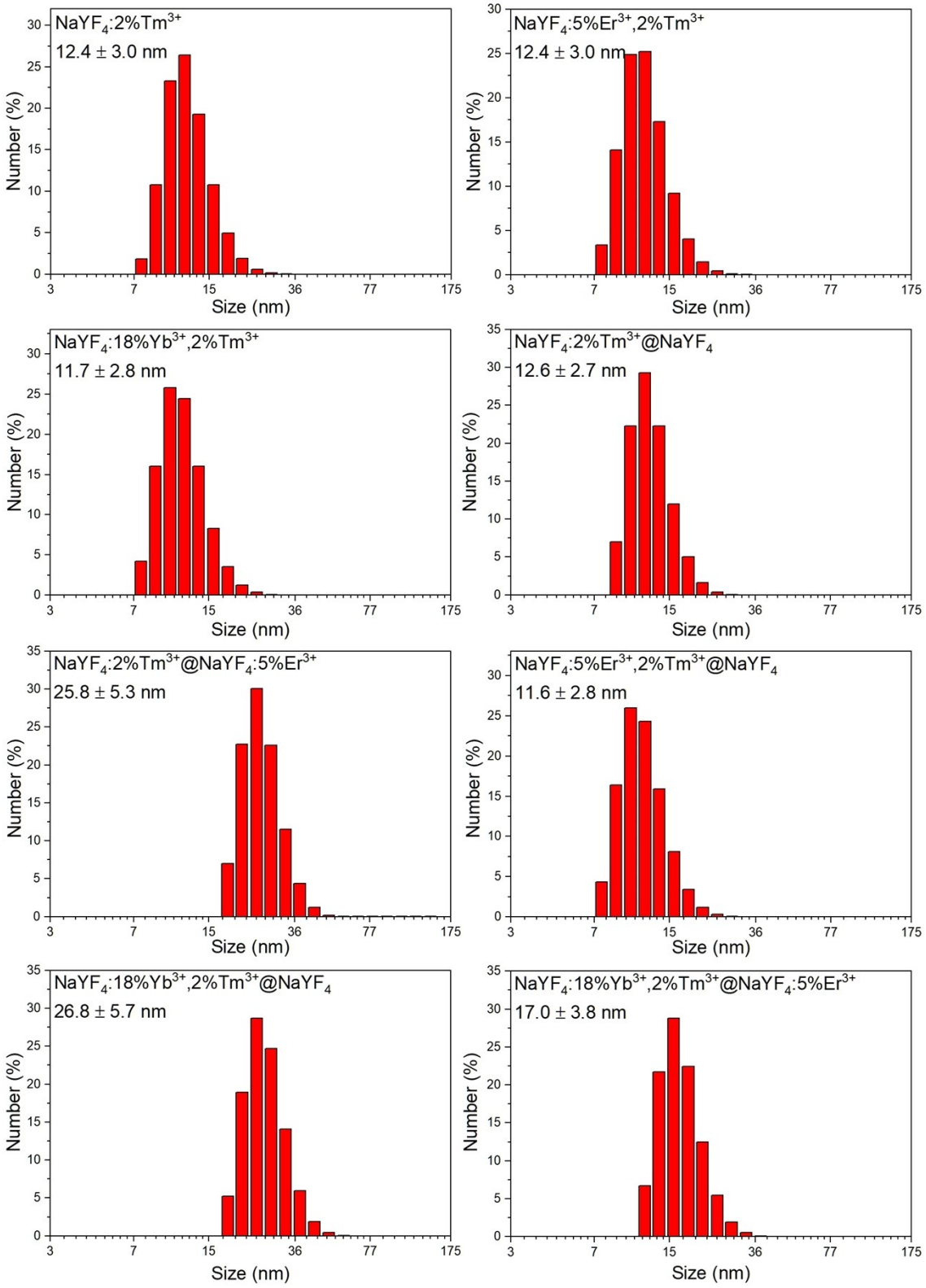

Fig. S3 Distribution of nanoparticle (NP) sizes, measured by DLS, in the form of hexane colloids.

3. Spectroscopic properties

The number of photons responsible for the observed up-conversion (UC) was determined based on the relationship between integral luminescence intensity (I_{UC}) and pumping laser power (I_p), which can be expressed by the equation:

$$I_{UC} = \alpha(I_P)^n \tag{2}$$

where α is a proportionality factor, and the exponent n represents the number of photons involved in the UC process.[2–4]

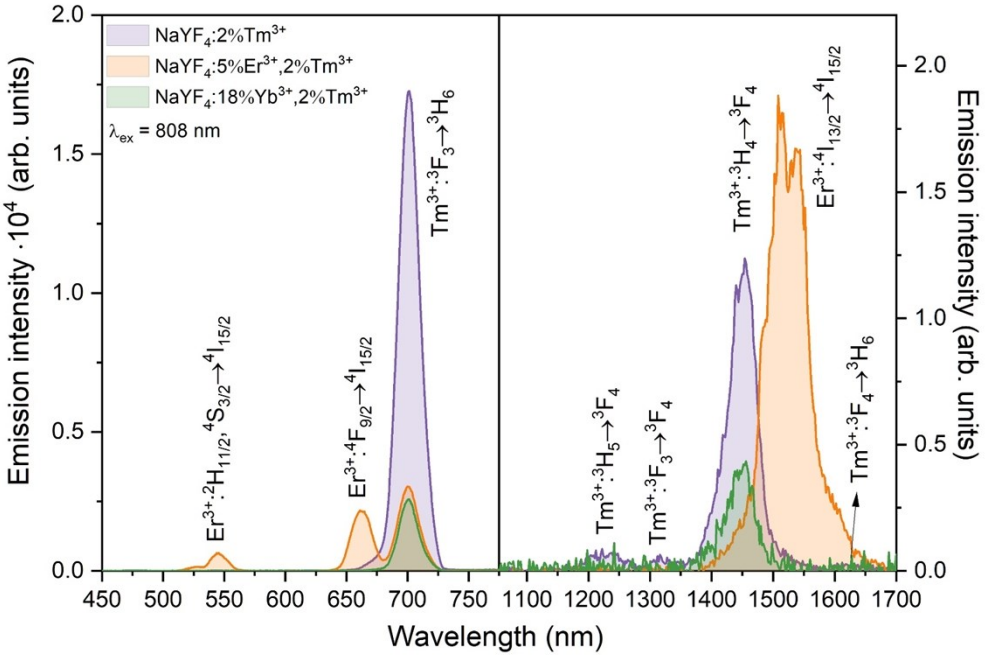

Fig. S4 Emission spectra of the core NPs in the visible (Vis) and near-infrared (NIR) range under excitation by 808 nm laser radiation (15 W·cm^{-2}). Left spectra were measured by CCD camera, whereas right spectra were recorded using a NIR PMT.

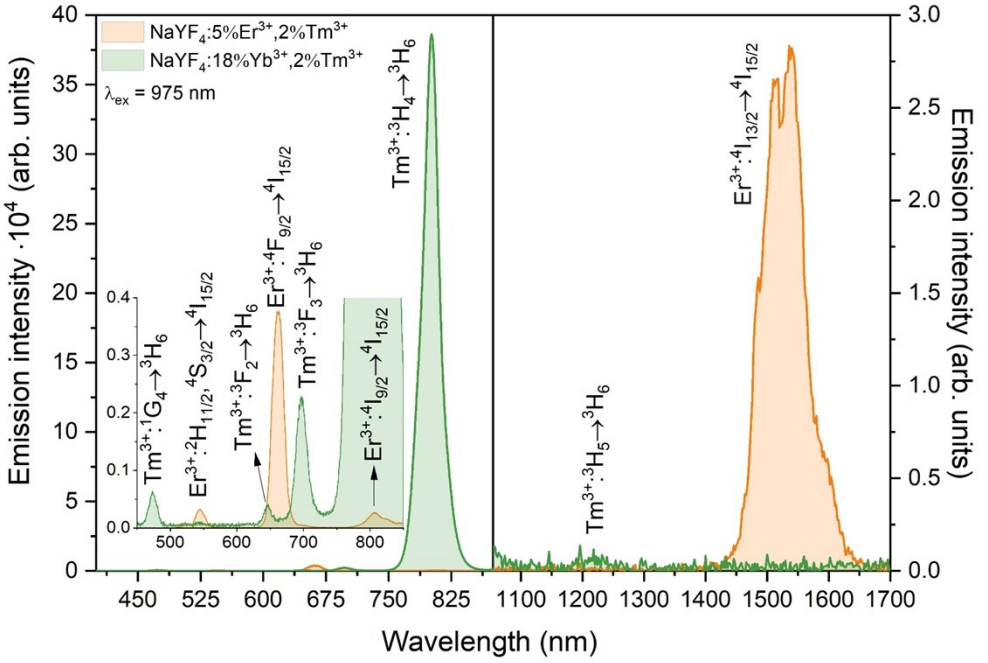

Fig. S5 Emission spectra of core NPs under excitation by 975 nm laser radiation (15 W·cm^{-2}). Left spectra were measured by CCD camera and right spectra with the use of a NIR PMT.

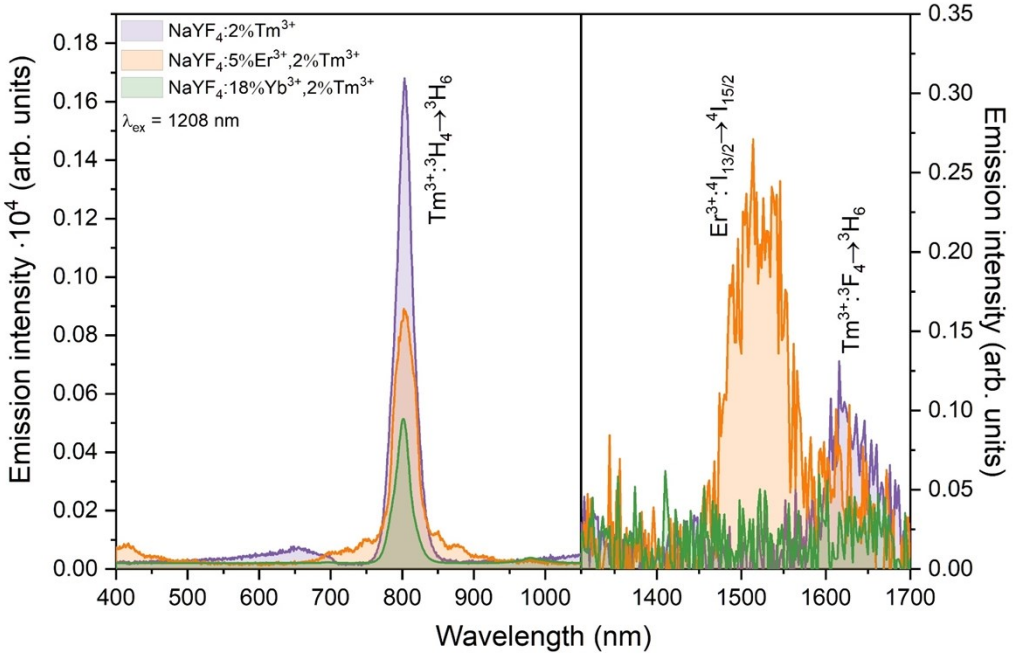

Fig. S6 Emission spectra of core NPs measured under excitation by 1208 nm laser radiation (15 W·cm^{-2}). Left spectra were measured by CCD camera and right spectra with use of an NIR PMT.

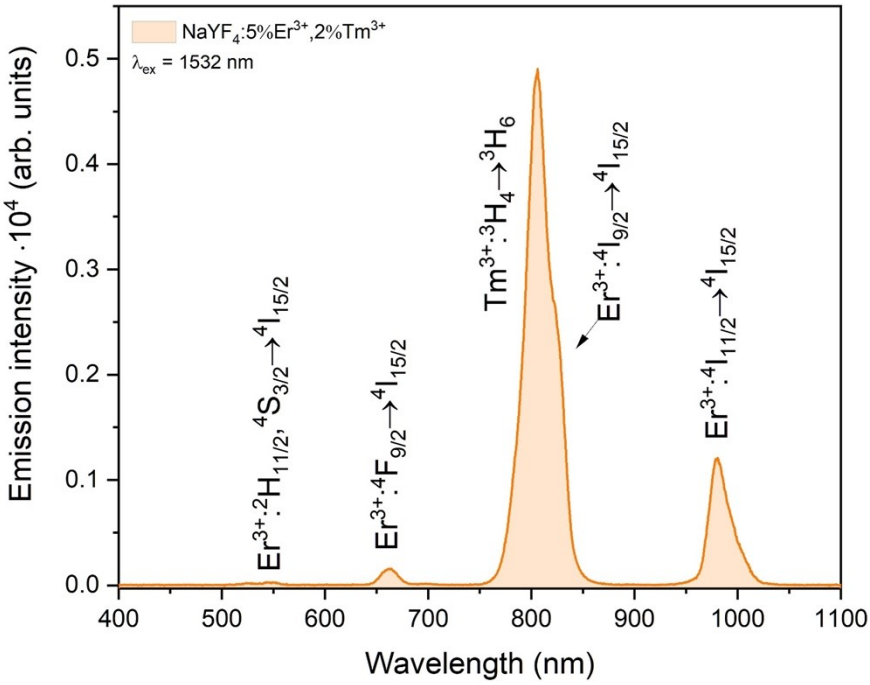

Fig. S7 Emission spectra of core NPs measured under excitation by 1532 nm laser radiation (15 W·cm^{-2}).

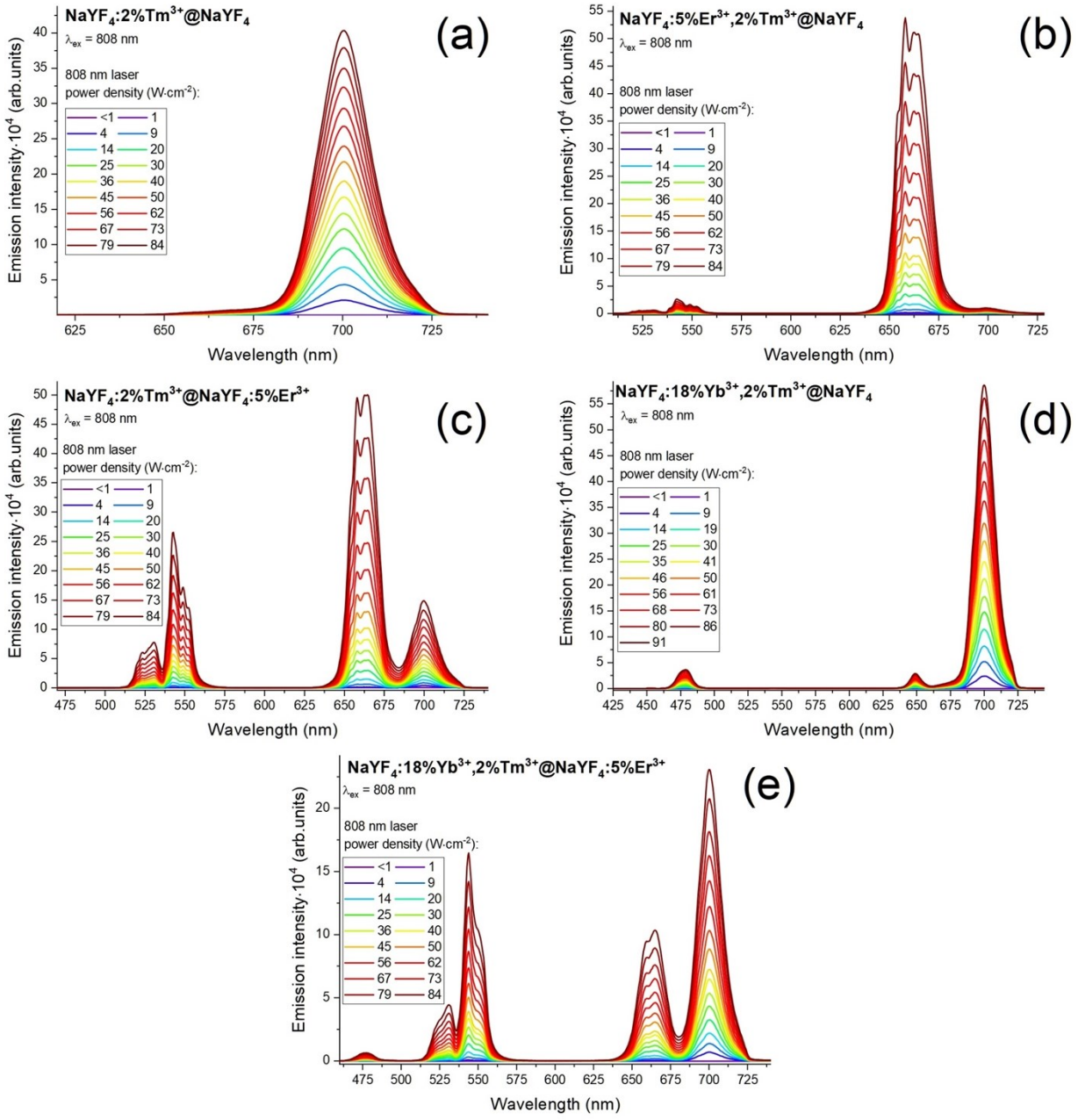

Fig. S8 Dependencies of the core@shell NPs emission intensities with 808 nm laser power density measured for (a) $NaYF_4$:2%Tm^{3+}@$NaYF_4$, (b) $NaYF_4$:5%Er^{3+},2%Tm^{3+}@$NaYF_4$, (c) $NaYF_4$:2%Tm^{3+}@$NaYF_4$:5%Er^{3+}, (d) $NaYF_4$:18%Yb^{3+},2%Tm^{3+}@$NaYF_4$ and (e) $NaYF_4$:18%Yb^{3+},2%Tm^{3+}@$NaYF_4$:5%Er^{3+} NPs.

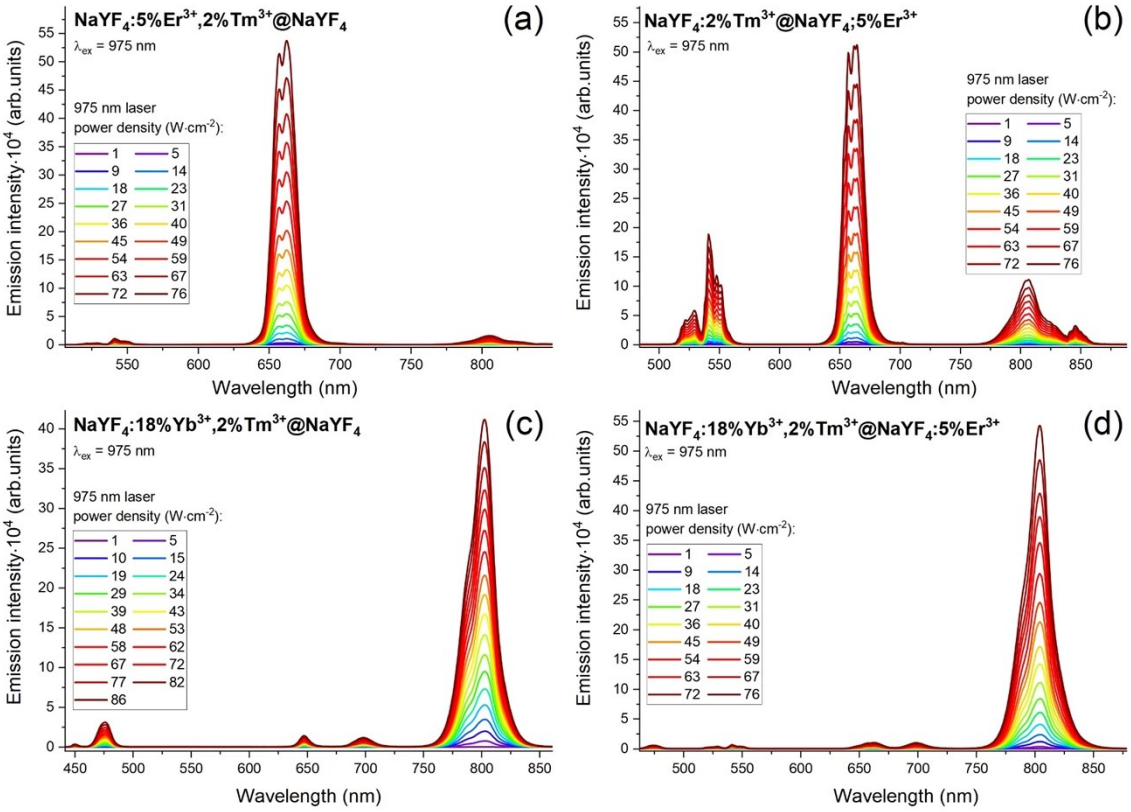

Fig. S9 Dependencies of the core@shell NPs emission intensities with 975 nm laser power density measured for (a) $NaYF_4$:5%Er^{3+},2%Tm^{3+}@$NaYF_4$, (b) $NaYF_4$:2%Tm^{3+}@$NaYF_4$:5%Er^{3+}, (c) $NaYF_4$:18%Yb^{3+},2%Tm^{3+}@$NaYF_4$ and (d) $NaYF_4$:18%Yb^{3+},2%Tm^{3+}@$NaYF_4$:5%Er^{3+} NPs.

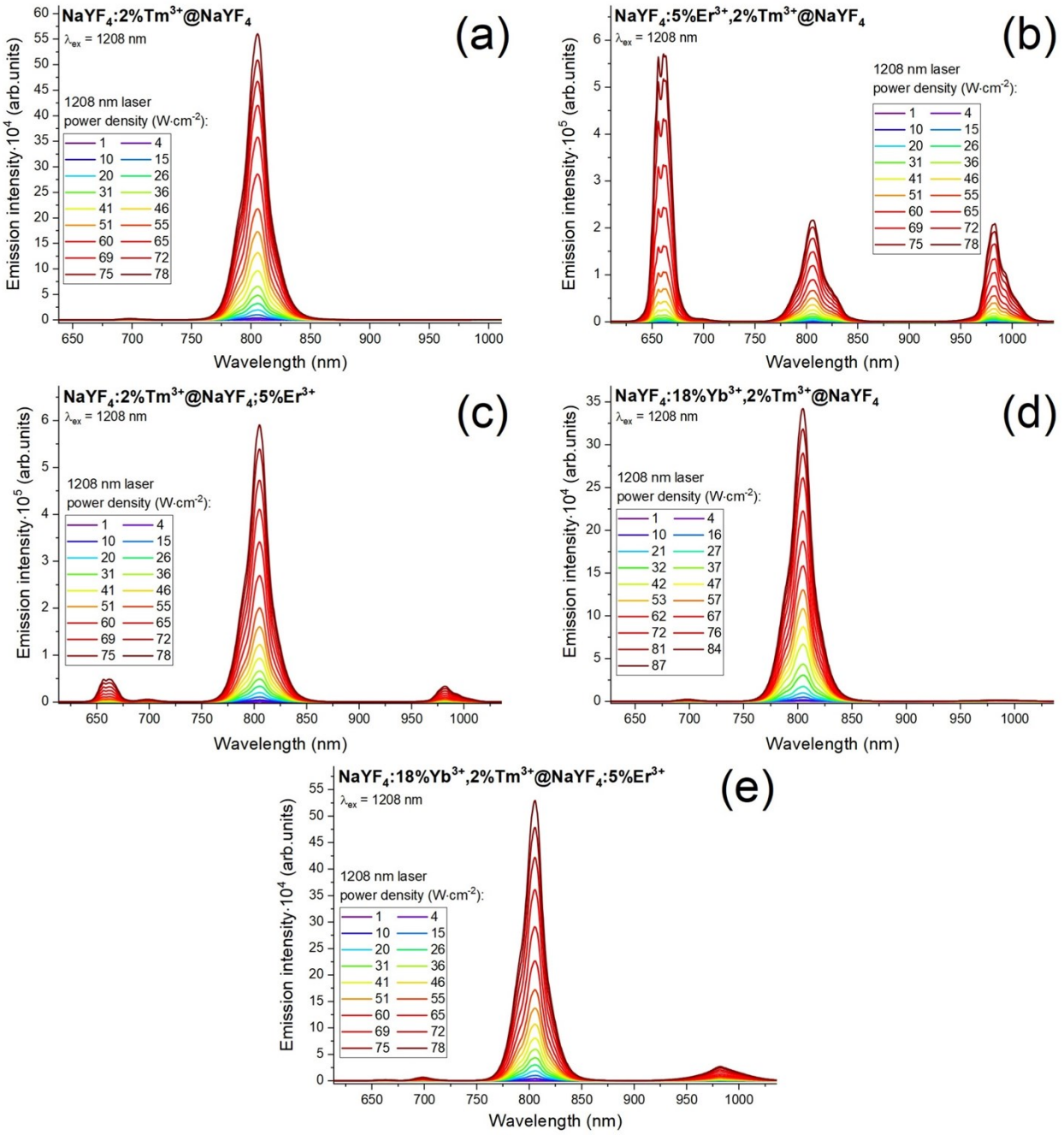

Fig. S10 Dependencies of the core@shell NPs emission intensities with 1208 nm laser power density measured for (a) $NaYF_4$:2%Tm^{3+}@$NaYF_4$, (b) $NaYF_4$:5%Er^{3+},2%Tm^{3+}@$NaYF_4$, (c) $NaYF_4$:2%Tm^{3+}@$NaYF_4$:5%Er^{3+}, (d) $NaYF_4$:18%Yb^{3+},2%Tm^{3+}@$NaYF_4$ and (e) $NaYF_4$:18%Yb^{3+},2%Tm^{3+}@$NaYF_4$:5%Er^{3+} NPs.

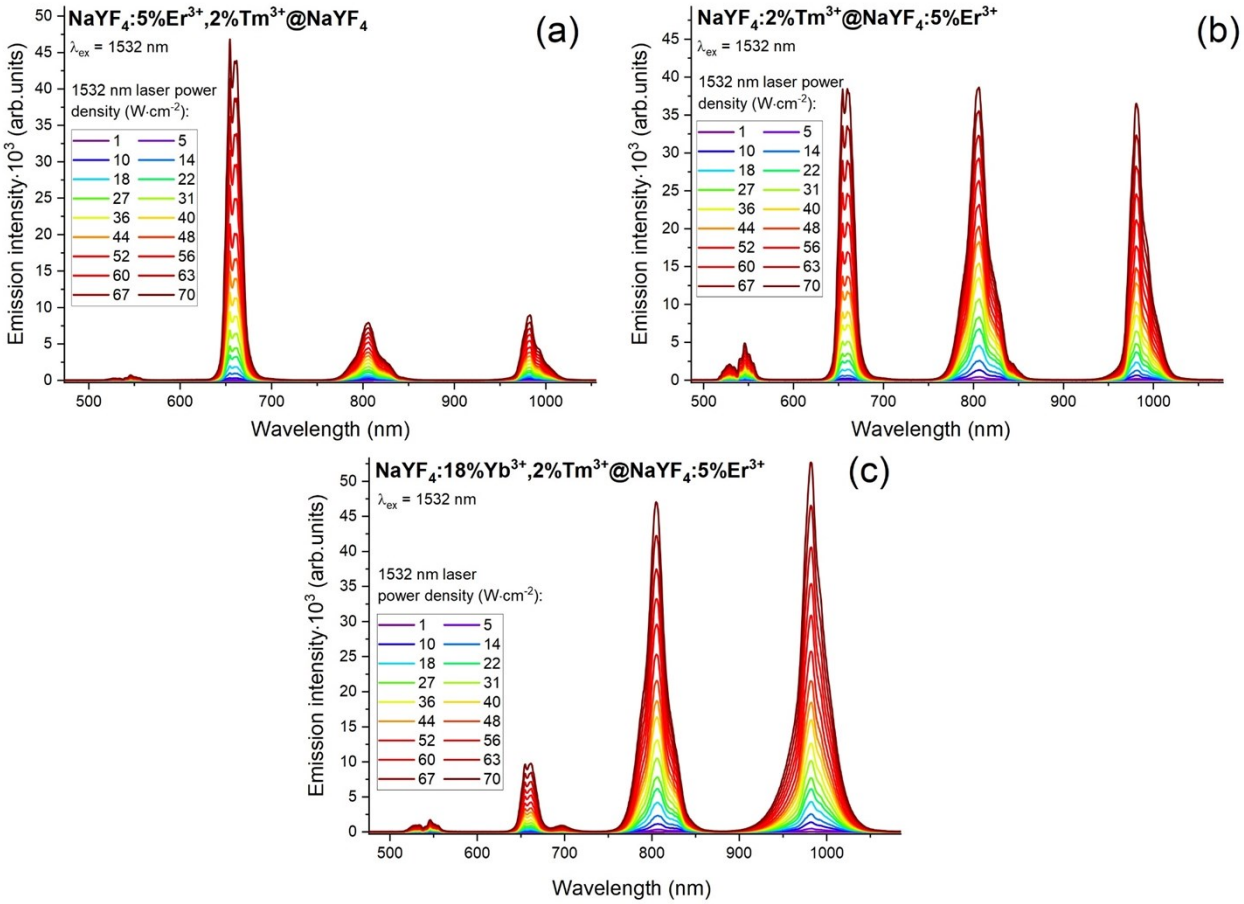

Fig. S11 Dependencies of core@shell NPs emission intensities with 1532 nm laser power density measured for (a) $NaYF_4$:5%Er^{3+},2%Tm^{3+}@$NaYF_4$, (b) $NaYF_4$:2%Tm^{3+}@$NaYF_4$:5%Er^{3+}, (c) $NaYF_4$:18%Yb^{3+},2%Tm^{3+}@$NaYF_4$:5%Er^{3+} NPs.

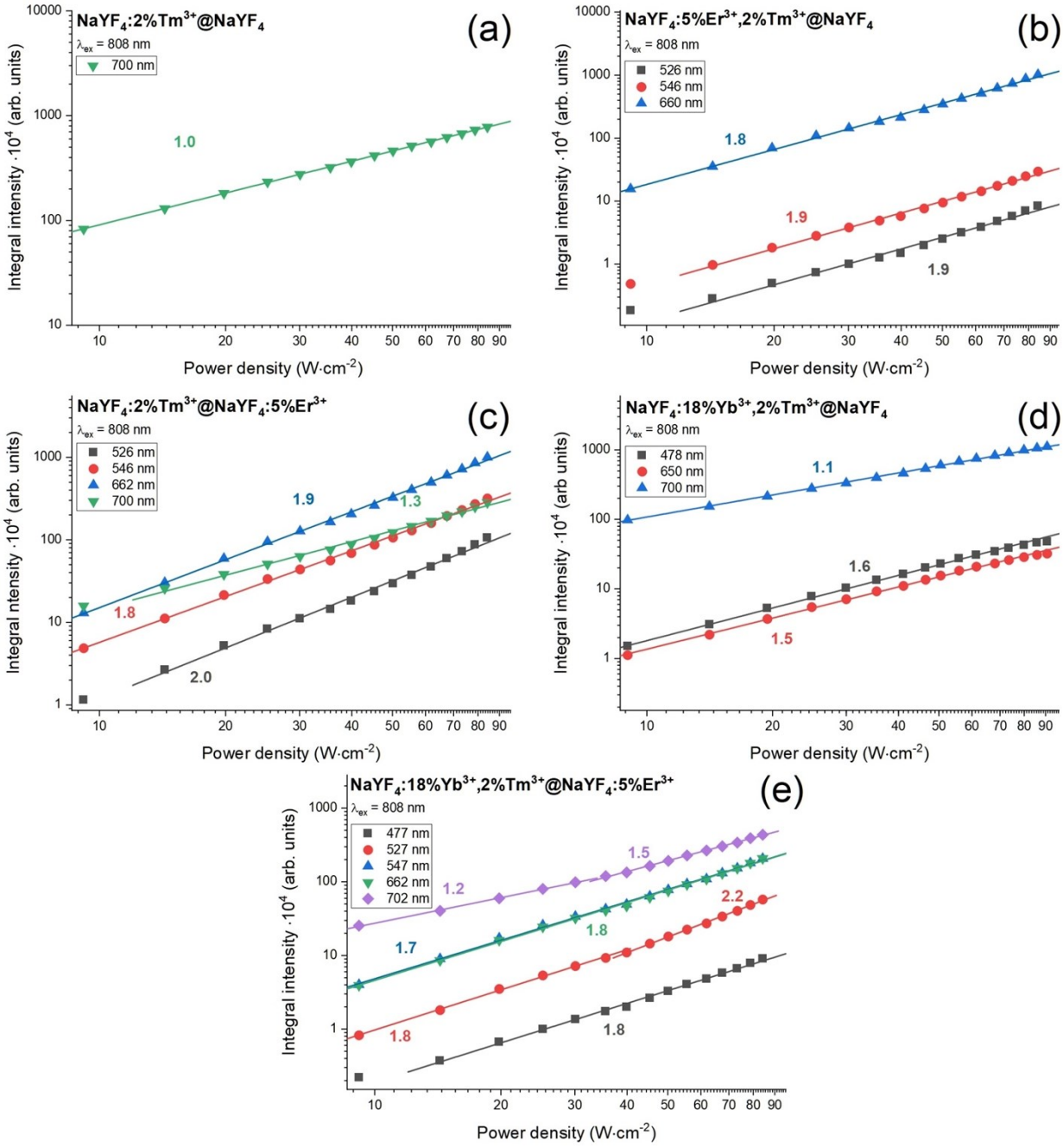

Fig. S12 Dependencies of UC integral intensity on laser power densities measured under excitation by 808 nm laser radiation determined for (a) $NaYF_4$:2%Tm^{3+}@$NaYF_4$, (b) $NaYF_4$:5%Er^{3+},2%Tm^{3+}@$NaYF_4$, (c) $NaYF_4$:2%Tm^{3+}@$NaYF_4$:5%Er^{3+}, (d) $NaYF_4$:18%Yb^{3+},2%Tm^{3+}@$NaYF_4$ and (e) $NaYF_4$:18%Yb^{3+},2%Tm^{3+}@$NaYF_4$:5%Er^{3+} NPs.

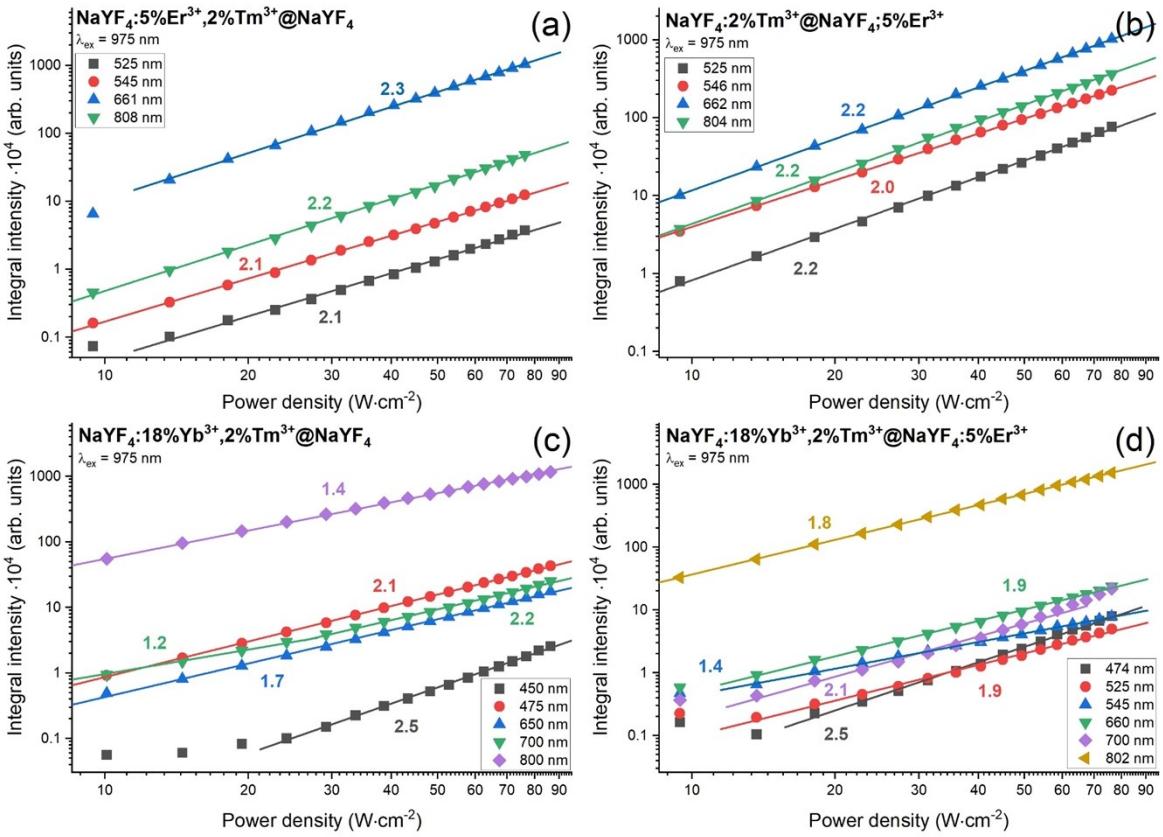

Fig. S13 Dependencies of UC integral intensity on laser power densities measured under excitation by 975 nm laser radiation determined for (a) $NaYF_4$:5%Er^{3+},2%Tm^{3+}@$NaYF_4$, (b) $NaYF_4$:2%Tm^{3+}@$NaYF_4$:5%Er^{3+}, (c) $NaYF_4$:18%Yb^{3+},2%Tm^{3+}@$NaYF_4$ and (d) $NaYF_4$:18%Yb^{3+},2%Tm^{3+}@$NaYF_4$:5%Er^{3+} NPs.

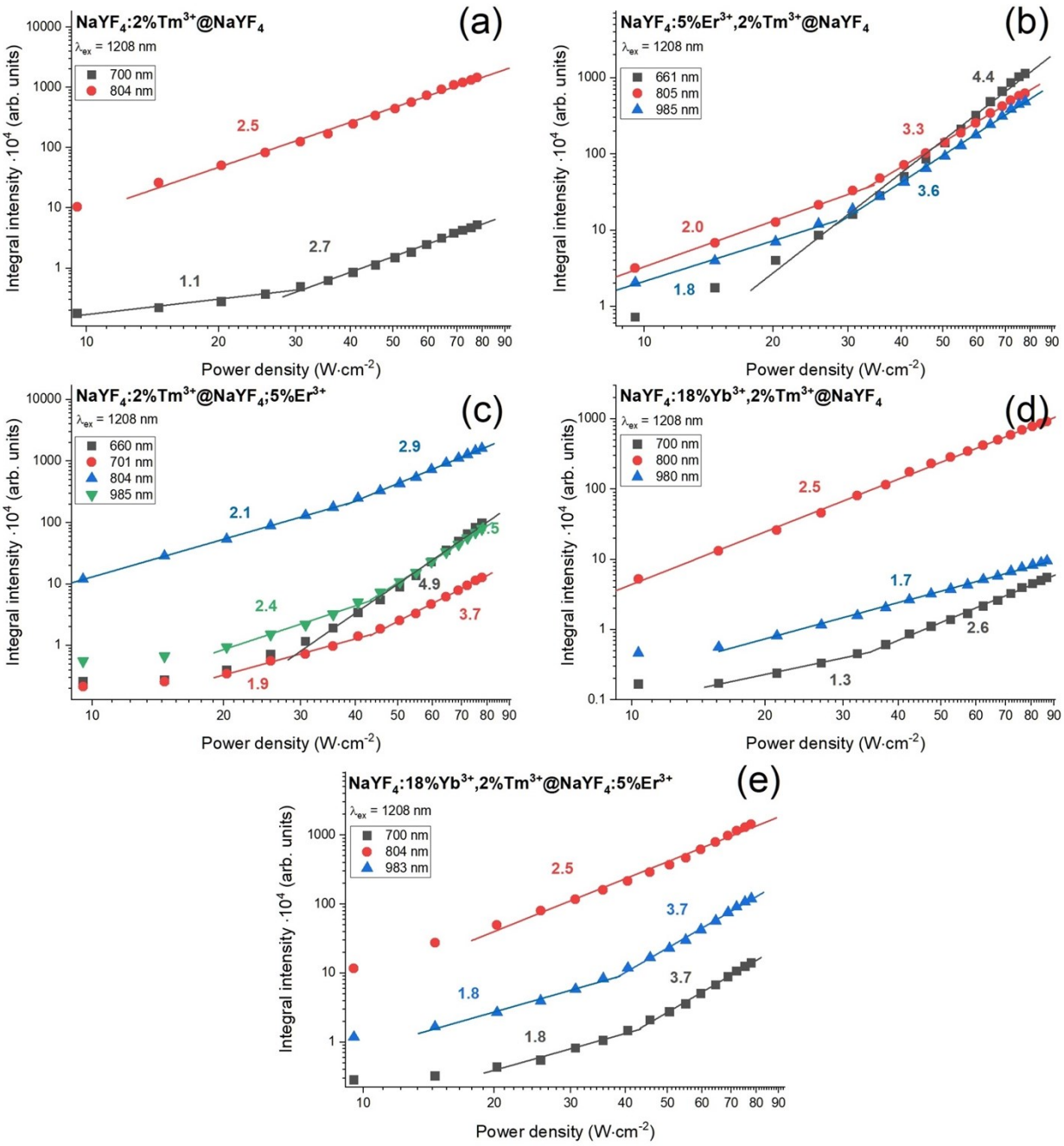

Fig. S14 Dependencies of UC integral intensity on laser powers measured under excitation by 1208 nm laser radiation determined for (a) $NaYF_4$:2%Tm^{3+}@$NaYF_4$, (b) $NaYF_4$:5%Er^{3+},2%Tm^{3+}@$NaYF_4$, (c) $NaYF_4$:2%Tm^{3+}@$NaYF_4$:5%Er^{3+}, (d) $NaYF_4$:18%Yb^{3+},2%Tm^{3+}@$NaYF_4$ and (e) $NaYF_4$:18%Yb^{3+},2%Tm^{3+}@$NaYF_4$:5%Er^{3+} NPs.

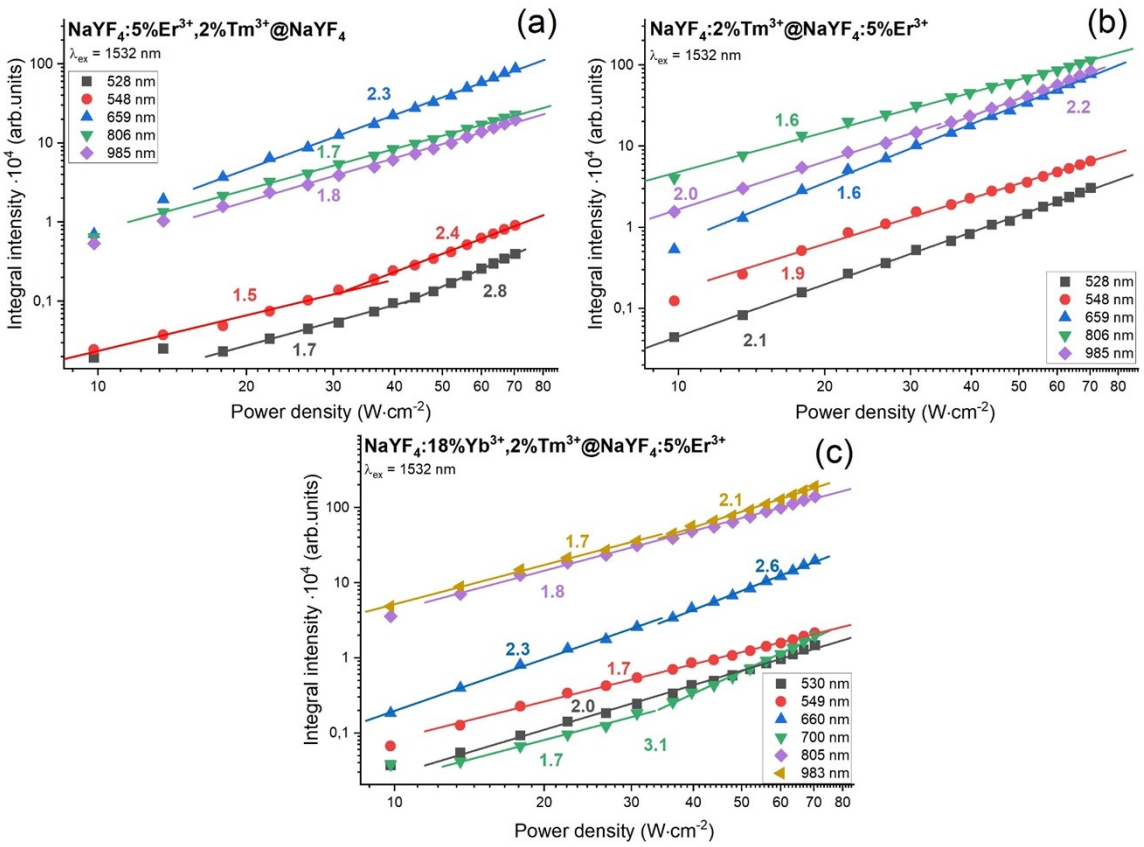

Fig. S15 Dependencies of UC integral intensity on laser powers measured under excitation by 1532 nm laser radiation determined for (a) $NaYF_4$:5%Er^{3+},2%Tm^{3+}@$NaYF_4$, (b) $NaYF_4$:2%Tm^{3+}@$NaYF_4$:5%Er^{3+} and (c) $NaYF_4$:18%Yb^{3+},2%Tm^{3+}@$NaYF_4$:5%Er^{3+} NPs.

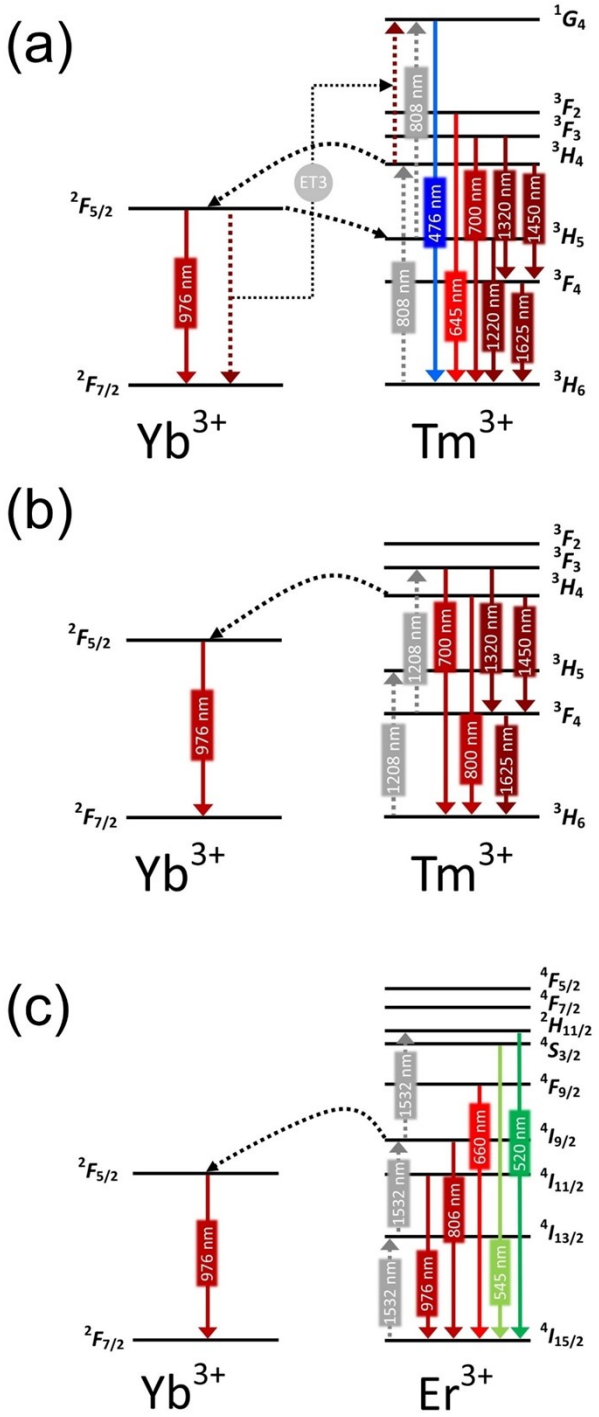

Fig. S16 Energy transfers in occurring in NPs containing Yb^{3+} in the structure, under excitation via (a) 808 nm, (b) 1208 nm, or (c) 1532 nm laser radiation.

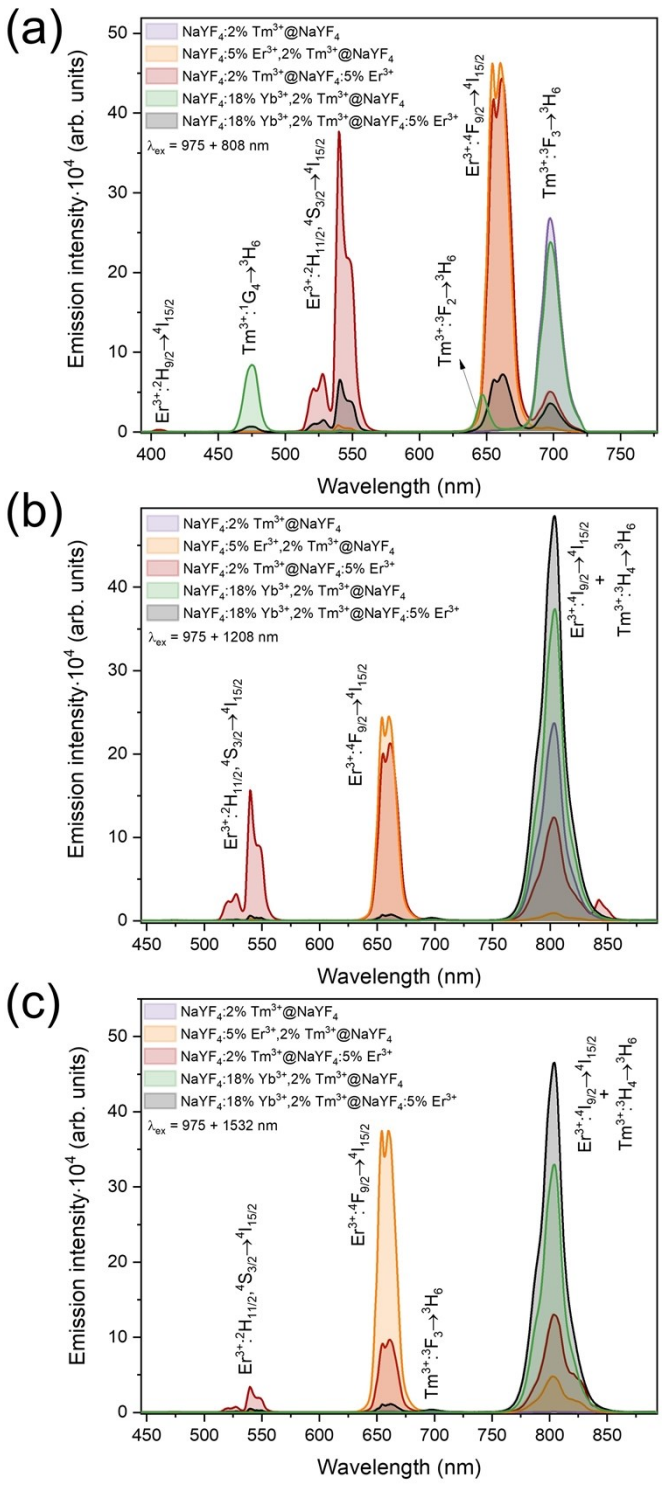

Fig. S17 Emission spectra of core@shell NPs measured under double-wavelength excitation: (a) 975+808 nm, (b) 975+1208 nm, (c) 975+1532 nm (7.5+7.5 W·cm^{-2}).

References

1 P. Scherrer, *Nachr. Ges. Wiss. Göttingen*, 1918, **26**, 98–100.

2 R. Scheps, *Ptog. Quant. Electron.*, 1996, **20**, 271–358.

3 M. Pollnau, D. Gamelin, S. Lüthi, H. Güdel and M. Hehlen, *Phys. Rev. B*, 2000, **61**, 3337–3346.

4 Y. Lei, H. Song, L. Yang, L. Yu, Z. Liu, G. Pan, X. Bai and L. Fan, *J. Chem. Phys.*, 2005, **123**, 174710.